

Prefouling Behavior of Suspended Particles in Petroleum Fluid Flow

J. Escobedo^{1,2} and G.A. Mansoori^{1,*}

Abstract. *The production and transportation of petroleum fluids will be severely affected by the deposition of suspended particles (i.e. asphaltenes, diamondoids, paraffin/wax, sand, etc.) in petroleum fluid production wells and/or transfer pipelines. In certain instances, the amount of precipitation is rather large causing complete fouling of these conduits. Therefore, it is important to understand the behavior of suspended particles during petroleum fluid flow conditions. In this paper, we present an analytical model for the prefouling behavior of suspended particles corresponding to petroleum fluids production conditions. We predict the rate of particle deposition during various turbulent flow regimes. The turbulent boundary layer theory and the concepts of mass transfer are utilized to model and calculate the particle deposition rates on the walls of flowing conduits. The developed model accounts for the eddy diffusivity and Brownian diffusivity as well as for inertial effects. The analysis presented in this paper shows that rates of particle deposition (during petroleum fluid production) on the walls of the flowing channel due solely to diffusional effects are small. It is also shown that deposition rates decrease with increasing particle size. However, when the process is momentum controlled (large particle sizes), higher deposition rates are expected.*

Keywords: *Asphaltene; Brownian diffusivity; Diamondoid; Fluid flow; Paraffin/wax; Particle deposition; Petroleum fluid; Prefouling behavior; Production operation; Sand; Suspended particles; Transport coefficient; Turbulent flow.*

INTRODUCTION

Production and transportation of petroleum fluids could be severely affected by the deposition of suspended particles (i.e. asphaltenes, diamondoids, paraffin/wax, sand etc.). In many instances, the amount of precipitation is rather large; causing complete fouling of flowing channels. Therefore, it is important to understand the behavior of the suspended particles during prefouling flow conditions.

Among all the suspended particles in petroleum fluid, asphaltene particles are more prone to fouling the flow conduits. Numerous experimental works have revealed the colloidal nature of the heavy asphaltene

fraction of a petroleum fluid. We consider the asphaltenes to exist in petroleum fluids as both dissolved and suspended particles [1-5]. In a petroleum fluid, dispersed asphaltene particles are, usually, sterically stabilized by neutral resins, they are electrically charged [6] and have a diameter of 3-4 nm [7]. The stability of these particles can be disrupted by addition of solvents (i.e. *n*-pentane); it could also be disrupted during flow conditions due to shear stresses or by counterbalancing the weak asphaltene particle charge. The latter is an important phenomenon, since, during petroleum fluid production a streaming potential is generated, which is believed to contribute to asphaltene aggregation [8]. When solvents are used to precipitate asphaltenes, the resulting aggregates may have a diameter as large as several hundred microns to become visible by laser particle counters [9]. In addition to asphaltenes, there may be other types of particle suspended in the petroleum fluid as well. For instance, sand particles swept from the reservoir matrix, paraffin crystals if the temperature falls below the cloud point of the crude and/or diamondoids.

1. *University of Illinois at Chicago, Chicago, IL, 60607-7052, USA.*

2. *Present address: Case Western Reserve University, 10900 Euclid Ave, Cleveland, OH 44106. E-mail: joescobedo1@gmail.com*

*. *Corresponding author. E-mail: mansoori@uic.edu*

Received 11 July 2009; received in revised form 24 September 2009; accepted 19 October 2009

This paper presents a theoretical analysis of Brownian diffusion and turbulent diffusion, and for inertial effects on the particle deposition with the utilization of the theories of Brownian motion, mass transfer and the boundary layer. The model presented here is intended to explain the prefoiling situation in regard to particle deposition on the walls of the well tubing (or pipeline). It accounts for Brownian and turbulent diffusion and for inertial effects.

THEORETICAL ANALYSIS

Substantial work has been reported in the literature in the area of particle deposition on the walls of channels or pipes in turbulent flow [10-18]. A key assumption in the development of the model reported here is that a fully developed turbulent flow of petroleum fluid has a structure as originally proposed by Lin et al. [10]. From experimental observations, they proposed a generalized velocity distribution for turbulent flow of fluids in pipes, as depicted in Figure 1, along with different flow regimes in the single-phase turbulent flow in the oil well. This velocity distribution is comprised of three main regions:

- A sublaminal layer adjacent to the wall,
- The transition or buffer region,
- The turbulent core [10].

In the sublaminal layer in which there is no turbulence or eddy diffusion, particle flux is due to Brownian diffusion. Velocity distribution and mass transfer in the turbulent core are governed primarily by eddy diffusivities; both of momentum and mass, whereas,

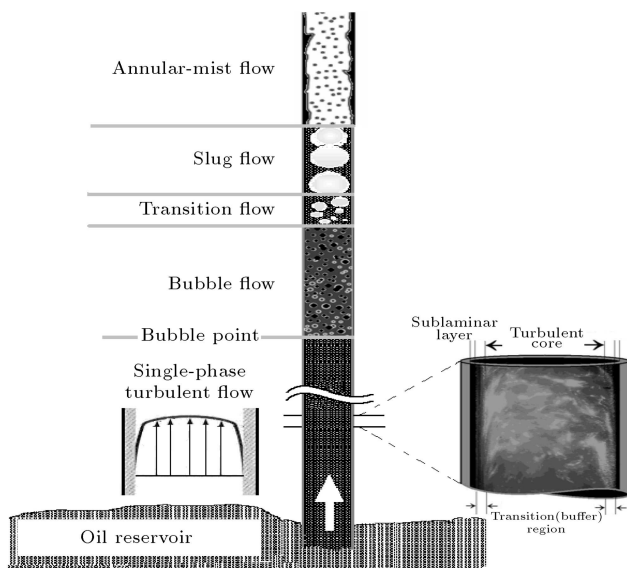


Figure 1. Illustration of velocity distribution and different flow regimes in the prefoiling single-phase turbulent flow condition in the oil well.

in the buffer region, mass transfer is governed by a combined action of Brownian and eddy diffusivities.

It has been observed experimentally that even in the sublaminal layer near the wall a slight amount of eddies is present [10]. However, it cannot be measured or correlated based on experimental observations. Nevertheless, empirical correlations have been proposed for eddy diffusivity in the turbulent boundary layer, as we use and as are presented below. These correlations are based on analogies with the laminar diffusion boundary layer [10,18].

The theoretical analysis that follows has been done for a system of constant density and viscosity. Therefore, it is applicable to the region above the bubble pressure where only the liquid phase is present. However, it could be extended to the region below the bubble point (gas-liquid slug flow etc.) if reliable correlations for viscosity and density versus pressure and composition are available. Because of the scarcity of such correlations, and because multi-phenomena occur in the two phase region of the well/tubing (i.e. release of the light ends of the crude, chemical composition variation, etc) that affect the diffusivity of the suspended particles, no attempt is made to extend this model to that region. The assumption of constant viscosity and constant density is partly justified since density changes are not appreciable until the bubble point pressure is reached inside the well (or tubing). It is also assumed that suspended particles are all with the same diameter, and that interactions between them are only due to their Brownian and eddy motion (i.e. we have neglected particle-particle interactions in the present paper).

If we assume that the thickness of the boundary layer is very small compared to the radius of the pipe, then we can neglect any curvature effects.

Thus, the equation used to describe the particle flux, N , in terms of the diffusivities and the concentration gradient is [19]:

$$N = (D_B + \varepsilon) \frac{dC}{dr}, \quad (1)$$

where D_B is the Brownian diffusivity; ε is the eddy diffusivity; C is the particles concentration and r is the radial distance. The Brownian diffusivity is expressed by the following equation:

$$D_B = \left(\frac{K_B T}{3\pi d \mu} \right),$$

where K_B is the Boltzmann constant (1.38066×10^{23} J/K); T is the absolute temperature; d is the particle diameter and μ is the viscosity of the suspending medium.

Equation 1 is subject to the boundary condition: at $r = S$ and $C = C_s$ where C_s is the particle

concentration at $r = S$ and S is the particle “stopping distance” measured from the wall.

A particle needs to diffuse only within one stopping distance from the wall and, from this point on, due to particle momentum it would coast to the wall. For small particles, the stopping distance is small compared to the boundary layer thickness and, consequently, diffusion dominates. The proposed expression for the particle stopping distance is [12]:

$$S = \frac{0.05\rho_p d^2 V_{\text{avg}} \sqrt{f/2}}{\mu} + \frac{d}{2}, \quad (2)$$

where ρ_p is density of particles; V_{avg} is the fluid average velocity and f is the friction factor. Equation 1 may be integrated following the procedure for the calculation of temperature drop across a composite wall. We will find the concentration profiles from point to point across the boundary layer. That is, we will calculate the concentration differences through the sublaminal layer, the buffer region and the turbulent core. By adding these concentration differences, we can find the overall particle flux in terms of the average and wall concentrations.

Before we integrate Equation 1 for C , we need to have expressions for N and ε as functions of the radial distance (r). Johansen [18] proposed the following correlation to express eddy diffusivity as a function of radial distance (r) for the sublaminal layer:

$$\varepsilon = \nu \left(\frac{r^+}{11.15} \right)^3 \quad r^+ \leq 5. \quad (3)$$

In this equation, ν is kinematic viscosity of the flowing fluid and r^+ is the dimensionless radial distance;

$$r^+ = \left(r V_{\text{avg}} \sqrt{f/2} \right) / \nu.$$

Note that Equation 3 is only valid for dimensionless radial distances smaller than 5, which is the limit of the sublaminal layer.

The molar flux, N , is assumed to vary linearly from the wall to the center line of the channel, as proposed by Beal [13]:

$$N = N_0 \left(1 - \frac{2r^+}{D_0^+} \right), \quad (4)$$

where N_0 is the particle flux at the wall and D_0^+ is the dimensionless well (or tubing) diameter;

$$D_0^+ = \left(D_0 V_{\text{avg}} \sqrt{f/2} \right) / \nu,$$

and D_0 is the inner diameter of the well (or tubing). In order to utilize Equations 3 and 4 in the integration of

Equation 1 for C , we must define another dimensionless variable;

$$s^+ = \left(s V_{\text{avg}} \sqrt{f/2} \right) / \nu,$$

called the dimensionless stopping distance. Introducing all the new dimensionless variables and the expressions for N and ε into Equation 1, we get:

$$\begin{aligned} N &= N_0 \left(1 - \frac{2r^+}{D_0^+} \right) \\ &= \left[\frac{D_B}{\nu} + \left(\frac{r^+}{11.15} \right)^3 \right] V_{\text{avg}} \sqrt{f/2} \frac{dC}{dr^+}, \end{aligned} \quad (5)$$

subject to the following boundary conditions:

$$\text{at } r^+ = s^+ \quad C = C_s^+,$$

$$\text{at } r^+ = 5 \quad C = C_5.$$

Rearranging Equation 5, integrating and applying the above boundary conditions, we find [2]:

$$\begin{aligned} C_5 - C_s^+ &= \frac{N_0}{V_{\text{avg}} \sqrt{f/2}} \left[\frac{11.15 S_c^{2/3}}{3} F_1(s^+, S_c) \right. \\ &\quad \left. + \frac{2(11.15)^2 S_c^{1/3}}{3D_0^+} F_2(s^+, S_c) \right]. \end{aligned} \quad (6)$$

In this equation $S_c = \frac{\nu}{D_B}$ is the Schmidt number and F_1 and F_2 are defined by the following expressions:

$$\begin{aligned} F_1(s^+, S_c) &= \ln \left[\left(\frac{1 + \frac{5}{11.15} S_c^{1/3}}{1 + \frac{s^+}{11.15} S_c^{1/3}} \right)^3 \left(\frac{1 + \left(\frac{s^+}{11.15} \right)^3 S_c}{1 + \left(\frac{5}{11.15} \right)^3 S_c} \right) \right]^{1/2} \\ &\quad + \sqrt{3} \tan^{-1} \left(\frac{\frac{10}{11.15} S_c^{1/3} - 1}{\sqrt{3}} \right) \\ &\quad - \sqrt{3} \tan^{-1} \left(\frac{\frac{2s^+}{11.15} S_c^{1/3} - 1}{\sqrt{3}} \right), \end{aligned} \quad (7)$$

$$\begin{aligned} F_2(s^+, S_c) &= \ln \left[\left(\frac{1 + \frac{5}{11.15} S_c^{1/3}}{1 + \frac{s^+}{11.15} S_c^{1/3}} \right)^3 \left(\frac{1 + \left(\frac{s^+}{11.15} \right)^3 S_c}{1 + \left(\frac{5}{11.15} \right)^3 S_c} \right) \right]^{1/2} \\ &\quad - \sqrt{3} \tan^{-1} \left(\frac{\frac{10}{11.15} S_c^{1/3} - 1}{\sqrt{3}} \right) \\ &\quad + \sqrt{3} \tan^{-1} \left(\frac{\frac{2s^+}{11.15} S_c^{1/3} - 1}{\sqrt{3}} \right), \end{aligned} \quad (8)$$

Equations 6 to 8 describe the transport of suspended particles to the wall in terms of the concentration difference between the limits $r^+ = s^+$ (dimensionless stopping distance) and $r^+ = 5$ (limit of the sublaminal layer).

The next step is calculation of the particle flux between the concentration at $r^+ = 5$ and $r^+ = 30$ (limit of the buffer layer). The eddy diffusivity expression for the buffer layer is assumed to be:

$$\varepsilon = \left[\left(\frac{r^+}{11.4} \right)^2 - 0.1923 \right] \nu$$

$$5 \leq r^+ \leq 30. \quad (9)$$

Integration of Equation 1, using Equation 9 for ε gives [2]:

$$C_{30} - C_5 = \frac{N_0}{V_{\text{avg}} \sqrt{f/2}} \left\{ 11.4 \left| \frac{S_c}{1 - 0.1923 S_c} \right|^{1/2} \right\}$$

$$[F_3(s^+, S_c)] - \frac{(11.4)^2}{D_0^+} \ln \left(\frac{1 - 0.1923 S_c + \left(\frac{30}{11.4} \right)^2 S_c}{1 - 0.1923 S_c + \left(\frac{5}{11.4} \right)^2 S_c} \right), \quad (10)$$

$$F_3(s^+, S_c) = \tan^{-1} \left(\frac{30}{11.4} \left| \frac{S_c}{1 - 0.1923 S_c} \right|^{1/2} \right)$$

$$- \tan^{-1} \left(\frac{5}{11.4} \left| \frac{S_c}{1 - 0.1923 S_c} \right|^{1/2} \right). \quad (11)$$

Equations 10 and 11 describe the particle transport in terms of the concentration difference between the limits of the buffer layer.

The following step is the calculation of the particle transport rate in terms of the difference between the concentration at $r^+ = 30$ (upper limit of the buffer layer) and the bulk concentration (average conc.). The eddy diffusivity for the turbulent core is taken to be [18]:

$$\varepsilon(0.4 r^+) \nu, \quad r^+ \geq 30. \quad (12)$$

If we assume that at $V = V_{\text{avg}}$ we have $C = C_{\text{avg}}$, then we could integrate Equation 1 using Equation 12 to obtain the following expression for C_{avg} [2]:

$$C_{\text{avg}} - C_{30} = \frac{N_0}{V_{\text{avg}} \sqrt{f/2}} \left[\left(2.5 + \frac{12.5}{D_0^+ S_c} \right) \right.$$

$$\left. \ln \left(\frac{2.5 r_{\text{avg}}^+ S_c}{2.5 + 30 S_c} \right) - \frac{5 r_{\text{avg}}^+}{D_0^+} + \frac{150}{D_0^+} \right]. \quad (13)$$

In this expression, r_{avg}^+ is the dimensionless ra-

dial distance (measured from the wall) where $V = V_{\text{avg}}$. Equation 13 describes the particle transport in terms of the concentration difference between the bulk (average) and the upper limit of the buffer layer.

So far we have expressions for the three different regions (wall layer, buffer layer, and turbulent core). Now, they may be added together to obtain an expression for N_0 , in terms of C_{avg} , C_S^+ , average fluid velocity, S^+ , and physical parameters of the system.

Until now, only dimensionless stopping distances (S^+) less than 5 have been considered. However, for particles large enough, S^+ could be greater than 5. If so, then the preceding analysis is not valid under these conditions. This difficulty may be overcome if Equation 1 is integrated between the limits $C = C_S^+$ at $r^+ = S^+$ and $C = C_{30}$ at $r^+ = 30$ using the eddy diffusivity correlation for the buffer layer as expressed by Equation 9.

Introducing Equation 9 into Equation 1 and integrating using the assumptions noted previously, we get [1,2]:

$$C_{30} - C_{s^+} = \frac{N_0}{V_{\text{avg}} \sqrt{f/2}} \left\{ 11.4 \left| \frac{S_c}{1 - 0.1923 S_c} \right|^{1/2} \right.$$

$$[F_3(s^+, S_c)]$$

$$\left. - \frac{(11.4)^2}{D_0^+} \ln \left(\frac{1 - 0.1923 S_c + \left(\frac{30}{11.4} \right)^2 S_c}{1 - 0.1923 S_c + \left(\frac{s^+}{11.4} \right)^2 S_c} \right) \right\}. \quad (14)$$

Such that:

$$F_3(s^+, S_c) = \tan^{-1} \left(\frac{30}{11.4} \left| \frac{S_c}{1 - 0.1923 S_c} \right|^{1/2} \right)$$

$$- \tan^{-1} \left(\frac{s^+}{11.4} \left| \frac{S_c}{1 - 0.1923 S_c} \right|^{1/2} \right). \quad (15)$$

If $s^+ = 5$, then Equations 14 and 15 reduce to Equations 10 and 11. Equation 13 still applies to the turbulent core.

For Particles with a Dimensionless Stopping Distance, $0 \leq S^+ < 5$

We add Equations 6, 10 and 13 to obtain an expression for the mass transfer (transport) coefficient defined as $N_0/(C_{\text{avg}} - C_S^+) = K$. K is the transport coefficient and has the dimension of velocity [cm/sec]. The expression for the transport coefficient obtained is [1,2]:

$$\begin{aligned}
 K = & V_{\text{avg}} \sqrt{f/2} \left[\frac{11.15 S_c^{1/3}}{3} F_1(s^+, S_c) \right. \\
 & + \frac{2(11.15)^2 S_c^{1/3}}{3D_0^+} F_2(s^+, S_c) \\
 & + 11.4 \left| \frac{S_c}{1 - 0.1923 S_c} \right|^{1/2} [F_3(s^+, S_c)] \\
 & - \frac{(11.4)^2}{D_0^+} \ln \left(\frac{1 + 6.7329 S_c}{1 + 0.000067 S_c} \right) \\
 & + \left(2.5 + \frac{12.5}{D_0^+ S_c} \right) \ln \left(\frac{2.5 r_{\text{avg}}^+ S_c}{2.5 + 30 S_c} \right) - \frac{5 r_{\text{avg}}^+}{D_0^+} \\
 & \left. + \frac{150}{D_0^+} \right]^{-1}. \quad (16)
 \end{aligned}$$

Parameters F_1 , F_2 and F_3 appearing in this equation are the same as defined previously by Equations 7, 8 and 11, respectively.

For Particles with a Dimensionless Stopping Distance, $5 \leq S^+ < 30$

We add Equations 13 and 14 and solving for K we get [1,2]:

$$K = \frac{V_{\text{avg}} \sqrt{f/2}}{\left[\begin{aligned} & 11.4 \left| \frac{S_c}{1 - 0.1923 S_c} \right|^{1/2} [F_3(s^+, S_c)] \\ & - \frac{(11.4)^2}{D_0^+} \ln \left(\frac{1 - 0.1923 S_c + \left(\frac{30}{11.4}\right)^2 S_c}{1 - 0.1923 S_c + \left(\frac{s^+}{11.4}\right)^2 S_c} \right) \\ & + \left(2.5 + \frac{12.5}{D_0^+ S_c} \right) \ln \left(\frac{2.5 r_{\text{avg}}^+ S_c}{2.5 + 30 S_c} \right) \\ & - \frac{5 r_{\text{avg}}^+}{D_0^+} + \frac{150}{D_0^+} \end{aligned} \right]}. \quad (17)$$

F_3 appearing in this equation is the same as previously defined by Equation 11.

Inertial Effects

In the above analysis, we have derived analytical expressions for the mass transport coefficient for different particle sizes, in terms of the dimensionless stopping distance.

Next, we must account for inertial effects. We use the following expression to account for inertial effects [13]:

$$K_D = \frac{N_0}{C_{\text{avg}}} = \frac{K p \vartheta}{K + p \vartheta}, \quad (18)$$

where K_D is the deposition coefficient (mass transfer coefficient) which contains the inertial effects, N_0 is

particle flux at the wall (as previously defined); p is the particle sticking factor (taken equal to unity); and ϑ is the average velocity of the particles near the walls, which consists of two parts:

$$\vartheta = \vartheta_f + \vartheta_B,$$

where ϑ_f is the particle velocity component due to fluid motion and ϑ_B is the component due to particle Brownian motion.

$$\vartheta_B = \left(\frac{K_B T}{2\pi m} \right)^{1/2},$$

$$\vartheta_f = \frac{V_{\text{avg}} \sqrt{f/2}}{4} [\vartheta_f^+(d^+/2) + \vartheta_f^+(S^+)],$$

where m is the particle mass, $\vartheta_f^+(d^+/2)$ is the particle velocity at dimensionless radial distance $d^+/2$; d^+ is the dimensionless particle diameter $\vartheta_f^+(S^+)$ is the particle velocity at dimensionless radial distance S^+ (dimensionless stopping distance) and the quantity ϑ_f^+ can be calculated using correlations proposed by Laufer [10]:

$$\vartheta_f^+ = 0.05 r^+ \quad \text{for } 0 \leq r^+ \leq 10,$$

$$\vartheta_f^+ = 0.5 + .0125(r^+ - 10) \quad \text{for } 10 \leq r^+ \leq 30.$$

The particles can be anywhere between $r^+ = d^+/2$ and $r^+ = S^+$. Considering this, we choose the appropriate expression for ϑ_f^+ .

The analysis for particle deposition onto the walls of a flowing channel from turbulent fluid streams is concluded by taking into account the inertial effects as in Equation 18. At this point, all the phenomena influencing the deposition rate (Brownian diffusivity, eddy diffusivity and inertial effects) have been taken into account.

COMPARISON OF THE PROPOSED MODEL WITH EXPERIMENTAL DATA AND OTHER MODELS

In order to apply the model developed above to particle deposition during turbulent flow production operations, we must compare the theoretical predictions against some experimental data. Unfortunately, experimental data for particle deposition from turbulent flows is very scarce and no data for deposition of particles from petroleum fluid is available. There is, however, more data for deposition from aerosols than from liquid suspensions. We make our comparisons here for particle deposition from turbulent gas streams. As shown below, the results of this analysis for particle deposition from turbulent fluid streams are in good

agreement with the experimental deposition rates [12] for iron particles in air. The predictions of the present model show a better agreement with the mentioned experimental data than the models proposed earlier.

Figure 2 shows a comparison of the proposed model predictions with the experimental data and two earlier models one in which Brownian diffusion was not taken into account [12] and the other in which Brownian diffusion was considered but it utilized different expressions for eddy diffusivities in the sublaminal layer and in the buffer region [13]. These calculations are for 800 nm diameter iron particles suspended in a turbulent air stream at 298 K inside a pipe with 0.54 cm inner-diameter.

As can be seen in Figure 2, there is very good agreement of the predicted deposition rates by the present model with the experimental data. The much better prediction capability of the present model is also noticeable compared to the earlier model [12] in which Brownian diffusion was not taken into account. It only takes into consideration particle momentum and eddy diffusion as the governing mechanisms for particle mobility.

In Figure 2, we also compare results of the present model predictions with the model proposed by Beal [13]. Although Beal's model takes into account Brownian diffusivity, it utilizes a less accurate correlation for eddy diffusivities in the sublaminal layer and in the buffer region. It also uses a less accurate correlation for the turbulent core. It can be seen from this figure

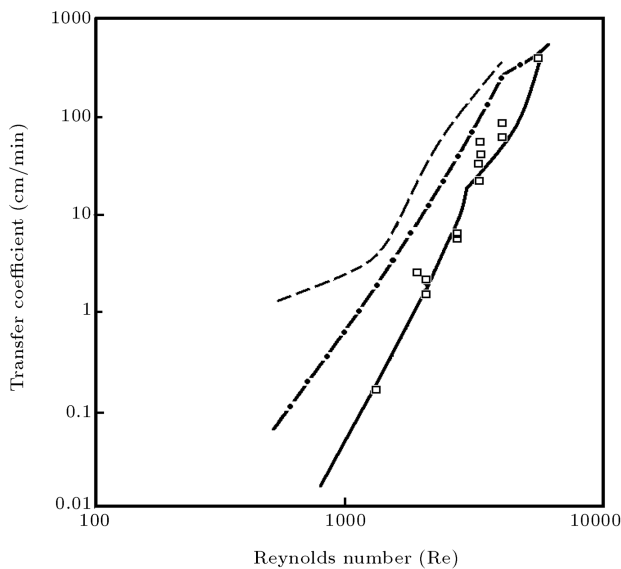


Figure 2. Comparison of the present model (solid line) with the experimental data and an earlier model [12] in which Brownian diffusion was not taken into account (dashed line) and model proposed by Beal [13] (dashed-dotted line) for 0.8μ iron particles suspended in a turbulent air stream with inner diameter of 0.54 cm and at 298 K.

that the proposed model has a much better prediction capability than the Beal model.

Overall, the reasons for the very good predictions by the present model are attributed to the fact that it takes into account Brownian diffusion as well as two other factors, namely particle momentum and eddy diffusivity, and considering more accurate correlations for eddy diffusivities and particle velocity. The reason we must consider Brownian diffusion is because the particles for which the data of Figure 2 are reported are small enough (800 nm) to be affected by Brownian motion phenomenon which cannot be ignored.

Figure 3 shows the experimental deposition coefficient data [12] for 800 nm and 1,570 nm iron particles suspended in a turbulent air stream at 298 K (pipe diameter is 1.3 cm). It also shows the experimental data for 1,810 nm diameter aluminum particles suspended in a turbulent air stream at 298 K (pipe diameter is 1.38 cm). From Figure 3, one can notice the very good prediction capabilities of the proposed model for all three sets of data.

In Figure 4, we examine the effect of particle diameter on the transport (transfer) coefficient at various Reynolds numbers. The results presented in this figure correspond to 800 nm iron particles suspended in flowing air at 298 K. As we can see from Figure 4, there is a dramatic decrease in the transport coefficient as the diameter of the pipe increases. This is not surprising, since the larger the diameter, the longer the distance particles have to travel prior to deposition.

We have also studied the effect of particle diameter on the transport coefficient for various Reynolds

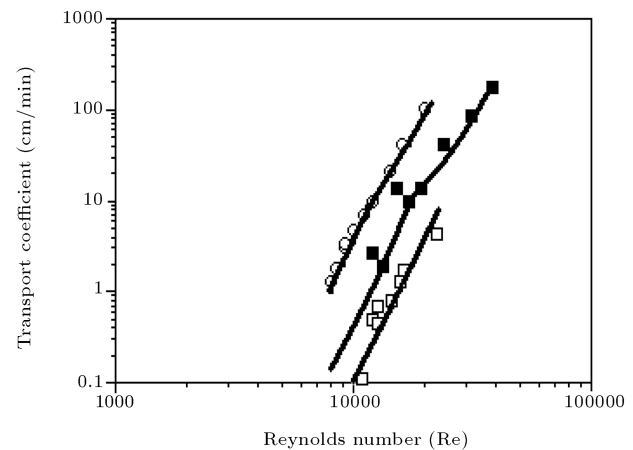


Figure 3. Comparison of the present model prediction (solid lines) with experimental data [12] for various particles suspended in turbulent flowing air in pipes. Circles are the data for 1,810 nm diameter aluminum particles (pipe diameter is 1.38 cm). Solid squares are the data for 800 nm diameter iron particles (pipe diameter is 1.3 cm). Empty squares are the data for 1,570 nm diameter iron particles (pipe diameter is 1.3 cm). All the data and calculations are at 298 K.

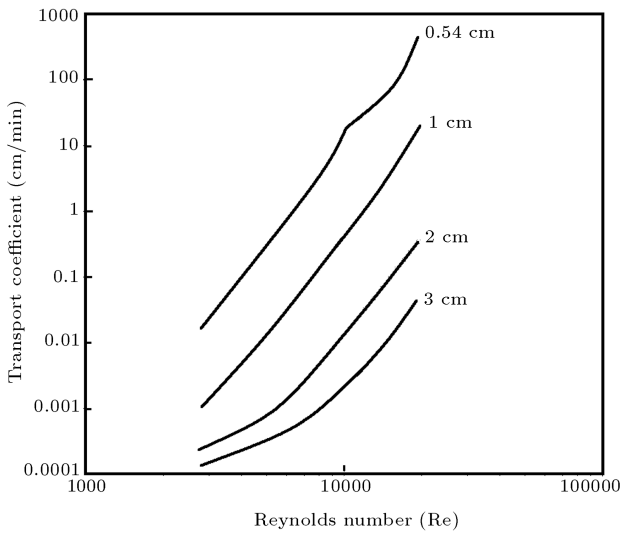


Figure 4. Prediction by the present model of the effect of Reynolds number and the inner pipe diameter on the transport (transfer) coefficient for 800 nm diameter iron particles suspended in a turbulent air stream at various Reynolds numbers.

numbers, as reported in Figure 5. These results were obtained for iron particles in air at 298 K flowing through a pipe of 0.54 cm inner diameter.

From this figure, we notice that the curves have the same shape as those predicted for Aitken nuclei, drops of tricresyl phosphate and polystyrene spheres, as reported by Beal [13]. There is no numerical data for these particles reported in Beal's paper, and no experimental data for iron particles are available. However, considering the very good success of the

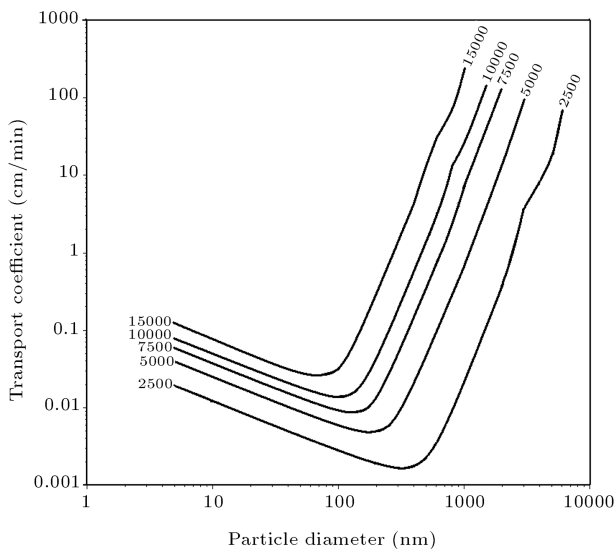


Figure 5. Prediction by the present model of the effect of particle diameter on the transport coefficient of iron particles suspended in turbulent air stream flowing through a pipe with an internal diameter of 0.54 cm and at various Reynolds numbers.

present model in accurate prediction for cases when data were available, we may conclude that this figure also represents actual conditions. From Figure 5, we notice a decrease in transport coefficient with increasing particle diameter and, at a certain particle diameter, a minimum is reached after which a sharp increase in the transport coefficient is observed. A physical explanation for this behavior is that, in the left-hand-side of the minima (small particles), the process is diffusion controlled, whereas in the right-hand-side of the minima (large particles), the process is momentum controlled.

MODEL PREDICTIONS FOR PARTICLE DEPOSITION INSIDE WELLS AND TUBINGS

Despite the good agreement of the present model predictions with the experimental data of iron and aluminum particles suspended in turbulent flowing air in pipes, it does not indicate that it could be applicable to predict the behavior of particles in turbulent petroleum fluid flow production operations. In order to justify the validity of the proposed model for this purpose, one has to determine, experimentally, the particle deposition coefficients in a turbulent petroleum fluid flow, and compare them with the model predictions. However, no experimental data is reported in the literature regarding this subject. Therefore, we believe the model is good enough to make, at least, qualitative predictions of the particle deposition coefficient from turbulent petroleum fluid flow, and is used as such.

Figure 6 shows the predicted transport coefficients for particles, as a function of particle diameter, for various petroleum fluid production rates.

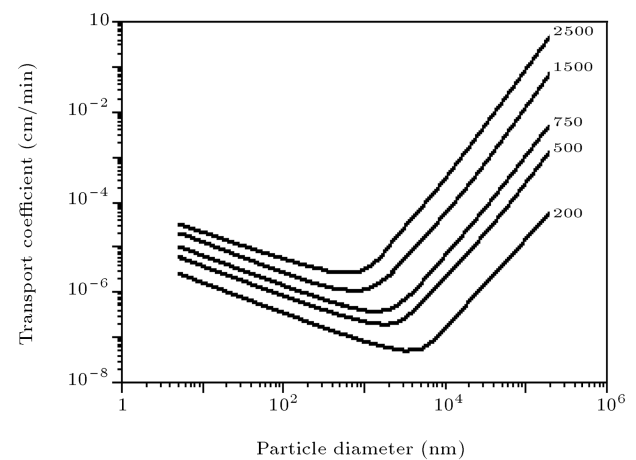


Figure 6. Prediction by the present model of the effect of particle size on the transport coefficient for a 30.21° API crude oil with a kinematic viscosity of 11 cSt at various production rates in (cu.m/day).

The particle sizes analyzed ranged from 5 to 200,000 nm. The results presented in this figure were obtained for a light petroleum fluid with 30.21°API (corresponding to 0.875 SG) and with a kinematic viscosity of 11 centi-Stokes. We notice from Figure 6 that the transport coefficients are generally small except at high production rates and for very large particles. As in Figure 5, we notice a minimum after which the transport coefficient increases more rapidly with increasing particle diameter. This is due to the fact that, at this point, the deposition process is momentum controlled. Judging from Figure 6, the amounts of particle deposition expected from turbulent petroleum fluid production may be very small when the diameter of the suspended particles is less than 1000 nm. However, higher amounts of deposition may be expected when the suspended particles have a diameter larger than 1,000 nm, especially at high production rates and when the turbulence is very high.

We performed model predictions varying the kinematic viscosity of the petroleum fluid to study the effect of this parameter on the deposition coefficient. Figure 7 shows the predicted values for a petroleum fluid containing suspended particles of 1,000 nm in diameter.

We can see a decrease in the deposition coefficients with increasing kinematic viscosity. This means that the lighter the petroleum fluid, the higher the probability of having particle deposition. We also notice an increase in the transport coefficient with increasing production rate. However, these predicted values are still very small.

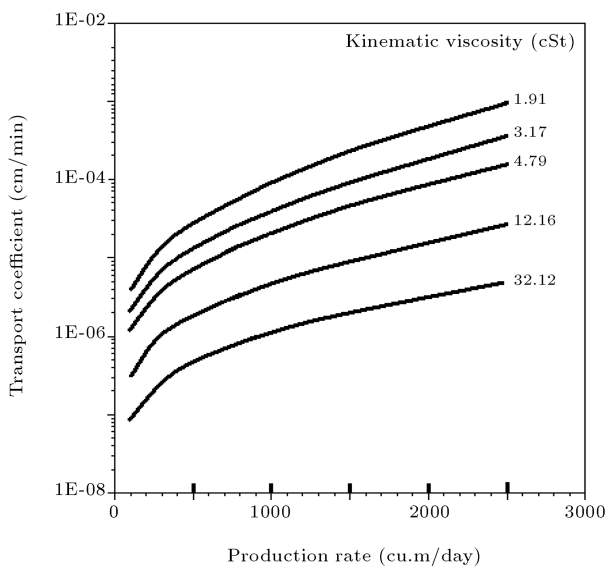


Figure 7. Prediction by the present model of the effect of petroleum production rate on the transport coefficient of 1 micron (1000 nm) in diameter suspended particles in crudes oils having various kinematic viscosities.

CONCLUSIONS

The model developed for the prefoiling conditions of particle deposition onto the walls of a pipe from a turbulent fluid stream shows fairly good agreement with the available experimental data. Furthermore, agreement with experimental data is better than the models proposed earlier by other investigators [12,13]. For these reasons, it can be used to predict the prefoiling transport coefficient from turbulent flow production operations. The effect of particle size on the transport coefficient was investigated, and it was found that when the deposition process is diffusion controlled (particles with diameter $< 1,000$ nm), the predicted values are very small. However, when the deposition process is momentum controlled (particles with diameters $> 1,000$ nm), the predicted values for the transport coefficient increase more rapidly with increasing particle diameter. We also investigated the effect of petroleum fluid kinematic viscosity on the transport coefficient. We found that transport coefficients decrease with increasing petroleum fluid kinematic viscosity. For kinematic viscosities 12.16 cSt, the predicted transport coefficients are negligible for suspended particles of 1,000 nm. We also found that transport coefficients increase with increasing production rate. This is due to the fact that, at larger production, the amount of eddy diffusion is bigger. The proposed model can be used for various cases of the prefoiling behavior of particle depositions from turbulent flows; whether it is asphaltene, paraffin/wax crystal or sand, so long as the particles are neutral, their sizes are stable, there are no particle-particle interactions and there are no phase transitions occurring in the flow. However, in cases where such changes are occurring in the system, this model will require appropriate modifications, as presented and applied elsewhere [20].

ACKNOWLEDGMENTS

The authors would like to thank Prof. Aly Hamouda of University of Stavanger and Professor Kamy Sephehrnouri and his colleagues and students at the University of Texas at Austin for taking time to read the manuscript and suggesting very useful corrections. To receive the executable computer package and the set of related equation for our proposed model please contact the corresponding author

REFERENCES

1. Escobedo, J. and Mansoori, G.A. "Asphaltene and other heavy-organic particle deposition during transfer and production operations", *SPE paper #30672, Proceed. Soc. of Petrol Eng. Annual. Tech. Conf. Held in Dallas, TX (22-25 Oct. 1995)*.

2. Escobedo, J. and Mansoori, G.A. "Solid particle deposition during turbulent flow production operations", *SPE paper #29488, Proceed. Soc. Petrol Eng. Production Operation Symp. Held in Oklahoma City, OK* (2-4 Apr. 1995).
3. Branco, V.A.M., Mansoori, G.A., De Almeida Xavier, L.C., Park, S.J. and Manafi, H. "Asphaltene flocculation and collapse from petroleum fluids", *J. Petrol Sci. & Eng.*, **32**, pp. 217-230 (2001).
4. Mousavi-Dehghani, S.A., Riazi, M.R., Vafaie-Sefti, M. and Mansoori, G.A. "An analysis of methods for determination of onsets of asphaltene phase separations", *J. Petrol Sci. & Eng.*, **42**(2-4), pp. 145-156 (2004).
5. Mansoori, G.A., Vazquez, D. and Shariaty-Niassar, M. "Polydispersity of heavy organics in crude oils and their role in oil well fouling", *J. Petrol. Sci. and Engineering*, **58**(3-4), pp. 375-390 (2007).
6. Lichaa, P.M. and Herrera, L. "Electrical and other effects related to the formation and prevention of asphaltene deposition in Venezuela", *Paper SPE paper #5304, Proceed. Soc. of Petrol Eng. Intl. Symposium on Oilfield Chemistry, Dallas TX* (Jan. 16-17, 1975).
7. Ray, R.B., Witherspoon, P.A. and Grim, R.E. "A study of the colloidal characteristic of petroleum using the ultracentrifuge", *J. Phys. Chem.*, **61**, pp. 1296-1302 (1957).
8. Katz, D.H. and Beu, K.E. "Nature of asphaltic substances", *Ind. Eng. Chem.*, **37**, pp. 195-200 (1945).
9. Eliassi, A., Modares, H. and Mansoori, G.A. "Study of asphaltene flocculation using particle counting method", *Proceed. Filtech 2005 (Int.'l Conf. & Exhib for Filtration & Separation Tech)*, **I**, pp. 506-511, Weisbaden, Germany (11-13 Oct. 2005).
10. Lin, C.S., Moulton, R.W. and Putnam, G.L. "Mass transfer between solid wall and fluid streams", *Ind. Eng. Chem.*, **45**, pp. 636-646 (1953).
11. Laufer, J. "The Structure of turbulence in fully developed pipe flow", *NACA 1174, National Advisory Committee for Aeronautics* (Available from NASA as TR-1174) (1954).
12. Friedlander, S.K. and Johnstone, H.F. "Deposition of suspended particles from turbulent gas streams", *Ind. Eng. Chem.*, **49**(7), pp. 1151-1156 (July 1957).
13. Beal, S.K. "Deposition of particles in turbulent flow on channel or pipe walls", *Nuclear Sci. Eng.*, **40**, pp. 1-11 (1970).
14. Derevich, I.V. and Zaichik, L.I. "Particle deposition from a turbulent flow", *Fluid Dynamics*, **23**(5), pp. 722-729 (1988).
15. Tandon, P. and Adewumi, M.A. "Particle deposition from turbulent flow in a pipe", *J. Aerosol. Sci.*, **29**(1-2) pp. 141-156 (1998).
16. Harriott, P. and Hamilton, R.M. "Solid-liquid transfer in turbulent pipe flow", *Chem. Eng. Sci.*, **20**, pp. 1073-1078 (1965).
17. Shapiro, M., Brenner, H. and Guell, D.C. "Accumulation and transport of Brownian particles at solid surfaces: Aerosol and hydrosol deposition processes", *J. Colloid Inter. Sci.*, **136**(2), pp. 552-558 (1990).
18. Johansen, S.T. "The deposition of particles on vertical walls", *Int. J. Multiphase Flow*, **17**(3), pp. 355-362 (1991).
19. Von Karman, T., *Aerodynamics: Selected Topics in the Light of Their Historical Development*, www.doverpublications.com (2004).
20. Mansoori, G.A. "ASPHRAC: A comprehensive package of computer programs and database which calculates various properties of petroleum fluids containing heavy organics", www.uic.edu/~mansoori/ASPHRAC.html